

# Strange Resonances and Exotic States

Anders G. Knospe<sup>1,\*</sup>

<sup>1</sup>Department of Physics, Lehigh University, Bethlehem, Pennsylvania, USA

**Abstract.** In these proceedings, I discuss how strange resonances and exotic states are used as unique probes in the field of ultrarelativistic heavy-ion physics. These particles can be used to study the properties of the hadronic phase of ion-ion collisions, the hadrochemistry of the system, flow and vorticity in the hot and dense medium, and the structures of the hadrons themselves. I provide an overview of recent results to illustrate these concepts.

## 1 Introduction

Strange hadronic resonances and exotic states provide a variety of ways to learn about the physics of heavy-ion collisions and about hadron structure. In these proceedings, I discuss a selection of experimental measurements and theoretical calculations, with an emphasis on recent results. The reader is invited to consult the cited presentations, proceedings, and papers for figures illustrating these results.

## 2 Resonance-to-Stable Yield Ratios & Hadronic Phase Properties

Measurements of resonance yields provide a way to study the properties of the later, post-hadronization phase of an ion-ion collision. Between chemical and kinetic freeze out, re-scattering and regeneration may modify the measurable yields of resonances; the strengths of these processes will be influenced by the properties of the hadronic phase (the temperatures at chemical and kinetic freeze out and the time interval between them), the lifetime of the resonance, and the scattering cross sections of its decay products. The  $K^*$  and  $\phi$  mesons are easily reconstructed resonances that have been used frequently to study these effects. The  $K^*/K$  yield ratio in central nucleus-nucleus collisions is observed to be suppressed with respect to the yields in peripheral  $A+A$  collisions, smaller collision systems (*e.g.*  $p+p$  and  $p+A$ ), and statistical thermal model calculations. [1, 2] This suggests that re-scattering is dominant over regeneration, leading to suppression of the  $K^*$  yield. This suppression has been observed at SPS energies, at RHIC energies (including in the Beam Energy Scan program) [3], and at the LHC. However, this suppression may vanish at low energies: NA61/SHINE observes no suppression of the  $K^{*0}/K$  ratio in Ar+Sc collisions at  $\sqrt{s_{NN}} = 8.8$  GeV (in comparison to  $p+p$  collisions at the same energy) [4]. They do, however observe suppression at higher collision energies; the lowest energy collisions may have a shorter-lived hadronic phase, which would result in less influence of re-scattering on the  $K^{*0}$  yield. In contrast, no suppression of the  $\phi/K$  yield ratio is observed in central  $A+A$  collisions. This is likely due to fact that the

---

\*e-mail: knospe@lehigh.edu

lifetime of the  $\phi$  meson ( $c\tau = 46.4$  fm/c) is an order of magnitude greater than that of the  $K^{*0}$  meson ( $c\tau = 4.17$  fm/c). The  $\phi$  lives longer than typical estimates of the hadronic phase lifetime, so its yield should not be affected strongly by re-scattering or regeneration. The  $\phi/K$  ratio appears to be independent of the colliding ions and of collision energy from  $\gtrsim 10$  GeV up to the top LHC energies. The  $K^*/K$  ratio depends on the system size, parameterized by the number of wounded nucleons, the number of participant nucleons, or the charged-particle multiplicity. When examined as a function of these quantities, the  $K^*/K$  and  $\phi/K$  ratios do not seem to depend on collision species or energy (*i.e.*, the  $K^*/K$  ratio at a given event multiplicity is quite similar for different collision energies or species) [3, 5]. This is true even when the ratios are measured as a function of multiplicity in  $p+p$  and  $p+\text{Pb}$  collisions. The resonance yields seem to be controlled primarily by the system size or multiplicity, an observation that also applies to long-lived hadron yields and strangeness enhancement. Theoretical models have had varying degrees of success at describing this behavior. EPOS uses UrQMD to model hadronic-phase effects and is able to qualitatively describe the observed suppression trends [6]. PHSD includes re-scattering and absorption of decay products in the hadronic phase; it can describe the observed  $K^*/K$  suppression trend [7]. MUSIC with the SMASH afterburner to describe the hadronic phase gives a  $K^*/K$  ratio that decreases with increasing collision centrality (although that decrease is less pronounced than seen experimentally), but MUSIC without SMASH does not exhibit such suppression [8]. The  $\gamma_S$  Canonical Statistical Model predicts only a slow decrease in the  $K^*/K$  ratio [9], while the Hadron Resonance Gas in Partial Chemical Equilibrium provides a good agreement with ALICE measurements of the  $K^*/K$  ratio. [10]

Under the assumption of simultaneous chemical freeze out of all long-lived hadron species and negligible regeneration of resonances,  $K^*/K$  ratio measurements can be used to estimate the time between chemical and kinetic freeze out. The lower limit on the hadronic phase lifetime  $\tau_{\text{low}}$  is extracted from the following expression:

$$\left(\frac{K^*}{K}\right)_{\text{kinetic}} = \left(\frac{K^*}{K}\right)_{\text{chemical}} \times \exp\left(-\frac{\tau_{\text{low}}}{\tau_{K^*}}\right). \quad (1)$$

The yield ratio in  $p+p$  collisions can be used as a proxy for the ratio at chemical freeze out, while the final measured yield ratio in a given centrality/multiplicity class is taken to be the ratio at kinetic freeze out. The extracted value for  $\tau_{\text{low}}$  is corrected by a Lorentz factor based on the mean momentum of the  $K^*$  mesons. Using this method, ALICE has estimated  $\tau_{\text{low}}$  values consistent with 0 for low-multiplicity  $p+p$  and  $p+\text{Pb}$  collisions, ranging up to approximately 6 fm/c in central Pb+Pb collisions [2]. This lifetime appears to depend on the charged-particle multiplicity, but not on the species of the colliding ions (for a given event multiplicity). ALICE has also performed a similar study using  $\Lambda(1520)$  baryons and  $\rho^0$  mesons. NA61/SHINE employed the same technique using  $K^*$  mesons to estimate the hadronic phase lifetime, which they found to be near 0 for  $\sqrt{s_{NN}} = 8.8$  GeV [4].

Other resonance-to-stable particle yield ratios can also be measured to shed light on the properties of the hadronic phase. Figure 1 (an updated version of a figure in [6]) is a summary of such measurements (see [1, 5] and the references listed in [6]). For clarity, only a selection of results are presented: the figure mostly shows ALICE  $p+p$ ,  $p+\text{Pb}$ , and  $\text{Pb}+\text{Pb}$  results, supplemented with analogous STAR results when necessary. These results are compared to EPOS calculations. Each resonance yield is divided by the yield of a long-lived hadron with similar quark content in order to cancel out strangeness enhancement or similar effects. The resonance lifetimes decrease from the top to the bottom of the figure. The  $\Xi^{*0}$  baryon lives about half as long as the  $\phi$  meson and may be expected to be somewhat more affected by re-scattering and/or regeneration. ALICE observes possible weak suppression of the  $\Xi^{*0}/\Xi^-$

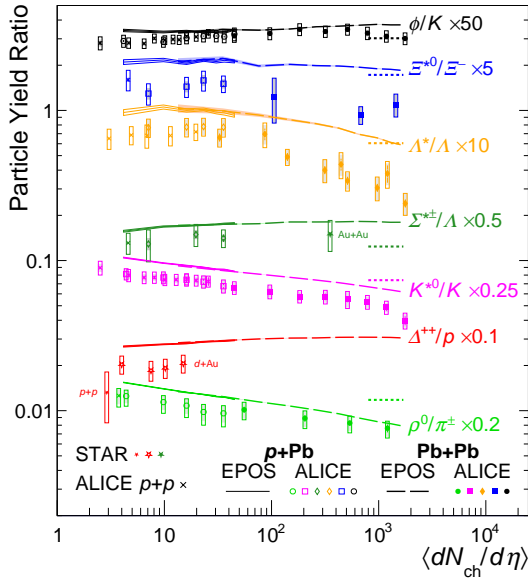


**Figure 1.** Summary plot showing a collection of particle yield ratios that illustrate the suppression trends for various resonances. Results from ALICE in small and large collision systems (supplemented by STAR data when necessary) are plotted as functions of the mid-rapidity charged-particle density and compared to EPOS calculations [6]. The ratios are scaled for visibility. The resonance lifetime decreases going from the top to the bottom of the plot. Bars represent statistical uncertainties, open boxes represent total systematic uncertainties, and shaded boxes represent systematic uncertainties that are uncorrelated between multiplicity/centrality classes. The experimental results come from [1, 5] and the references listed in [6].

ratio in (mid-)central  $A+A$  collisions. The  $\Lambda(1520)$  baryon has a lifetime about 3 times shorter than the  $\phi$  and 3 times longer than the  $K^{*0}$ . The  $\rho^0$  meson has a significantly shorter lifetime than  $K^{*0}$ . Both of these exhibit clear suppression trends with increasing centrality in  $A+A$  collisions, qualitatively similar to the trend seen for  $K^*/K$ . The suppression or non-suppression trends of the resonances mentioned so far can be at least qualitatively described by EPOS. However, resonance suppression may depend on properties other than the lifetime. The  $\Sigma^*$  and  $\Delta$  baryons have lifetimes similar to or smaller than the  $K^*$  meson. Despite these short lifetimes, EPOS predicts no suppression (and, in fact, a small enhancement) of the  $\Sigma^*/\Lambda$  and  $\Delta/p$  ratios with increasing system size. Measurements of these resonances are unfortunately difficult, particularly in  $A+A$  collisions. The STAR measurement of the  $\Sigma^*/\Lambda$  ratio exhibits no suppression trend. ALICE sees hints of possible weak suppression of the  $\Sigma^*/\pi^\pm$  yield ratio in  $A+A$  collisions [11], but ALICE has not published final measurements of the  $\Sigma^*/\Lambda$  ratio. Publication of that result, measurements of the  $\Delta$  baryon in  $A+A$  collisions, or measurements of other resonance species could help us improve our picture of the hadronic phase.

### 3 Hadrochemistry

Resonances including the  $\phi$  meson can also be used to study other aspects of the hadrochemistry of the collision system, shedding light on how hadron yields are affected by the properties of the medium and the hadron. ALICE recently released a comprehensive study of hadron production as a function of transverse sphericity [12]. For the 0–10% highest multiplicity  $p+p$  collisions at  $\sqrt{s} = 13$  TeV, ALICE split the data sample into sphericity classes, ranging from very jet-like to very isotropic. ALICE observes that the production of hadrons with open strangeness, like  $\Xi$ , is suppressed in jet-like collisions. This suggests that strangeness enhancement is connected to the properties of the underlying even and soft processes. However,  $\phi$  meson production is observed to be independent of sphericity in this study, suggesting that the  $\phi$  behaves like a particle that contains no strange quarks. This is in contrast to studies of the evolution of the  $\phi/\pi$  yield ratio with event multiplicity. The  $\phi/\pi$  ratio is observed to increase with multiplicity [13]; this increase appears to be more pronounced than the increases of the  $K/\pi$  and  $\Lambda/\pi$  ratios, but smaller in magnitude than the increase in the

$\Xi/\pi$  ratio. This suggests that the  $\phi$  meson may behave as if it has an effective strangeness content between 1 and 2 units. Further theoretical investigations are likely needed to reconcile this with the aforementioned sphericity study.

Other interesting results come from studies of  $\phi$  meson production at low energies. NA49 and NA61/SHINE observe that the  $\phi/\pi$  yield ratio increases with collision energy over the range  $5 \lesssim \sqrt{s_{NN}} \lesssim 20$  GeV [14]. This increase is seen in large and small collisions and may be attributable to strangeness enhancement. The  $\phi/K$  yield ratio has also been measured in A+A collisions at energies  $\sqrt{s_{NN}} \lesssim 3$  GeV, below the  $\phi$  production threshold for  $p+p$  collisions. While the  $\phi/K$  yield ratio is essentially constant from top SPS energies up to LHC energies, HADES, FOPI, and STAR observe that the  $\phi/K$  ratio is higher in this sub-threshold regime than it is at larger energies [15]. This is likely due to the canonical suppression of the kaon yields. These measurements can be used to estimate the correlation radius  $R_C$  in canonical statistical models, although there is currently a discrepancy in the  $R_C$  values extracted from the  $\phi/K^-$  and  $\phi/\Xi$  yield ratios. Theoretical frameworks including UrQMD and PHSD have had some success in describing this behavior.

## 4 Hadron Structure

Recent measurements of  $f$  and  $a$  mesons and excited kaons have the potential to provide information about the structure of those hadrons. These mesons may have simple  $q\bar{q}$  structures or they may have more exotic structures. Among the possibilities are hybrid mesons (containing valence gluons and quarks), glueballs, meson-meson molecules, and other tetraquark configurations. ALICE has measured the  $f_0(980)/\pi$  yield ratio in  $p+p$  collisions [16]. This measurement is compared to two different implementations of the canonical statistical model [9], one assuming that the  $f_0(980)$  is a  $s\bar{s}$  state (the  $|S| = 2$  hypothesis) and the other assuming that  $f_0(980)$  is a  $q\bar{q}$  meson with no  $s\bar{s}$  content (the  $|S| = 0$  hypothesis). The measured  $f_0(980)/\pi$  ratio is in better agreement with the  $|S| = 0$  hypothesis. ALICE also observes that the  $f_0(980)/K^{*0}$  ratio decreases with increasing multiplicity in  $p+Pb$  collisions [17]. This suppression is described by the  $\gamma_S$  Canonical Statistical Model with the  $|S| = 0$  hypothesis; the  $|S| = 2$  hypothesis predicts a slow increase in the  $f_0(980)/K^{*0}$  ratio with multiplicity. ALICE measurements of the  $f_0(980)$  nuclear modification factor in  $p+Pb$  collisions do not exhibit Cronin enhancement, which is taken to support the hypothesis that this meson has a simple quark-antiquark structure. CMS has measured the  $v_2$  elliptic flow parameter of  $f_0(980)$  in  $p+Pb$  collisions [18]. By performing  $n_q$  scaling with a variable number of constituent partons, they found that the preferred  $n_q$  value is near 2, strongly favoring a simple quark-antiquark structure for  $f_0(980)$ .

ALICE has measured the  $f_1(1285)$  meson in  $p+p$  collisions [19]. The measured  $f_1(1285)/\pi$  ratio is better described by the  $\gamma_S$  Canonical Statistical Model with the  $|S| = 0$  hypothesis [9], suggesting little hidden strangeness content for this meson. ALICE has measured the correlation functions for  $K_S^0 K_S^0$  pairs (which can originate from  $f_0(980)$  decays) and  $K_S^0 K^\pm$  pairs (which can originate from  $a_0(980)^\pm$  decays) [20]. While the correlation radius  $R$  is the same for both types of pairs, the correlation strength  $\lambda$  is significantly smaller (by about a factor of 2) for  $K_S^0 K^\pm$  pairs, suggesting that the  $a_0(980)^\pm$  may be a tetraquark. ALICE has also measured the correlation function for  $K_S^0 \pi^\pm$  pairs, which may originate from  $K_0^{*0}(700)^\pm$  decays [21]. The correlation strength  $\lambda$  is observed to increase as a function of the correlation radius  $R$ , which is consistent with a tetraquark configuration.

## 5 Flow & Vorticity

$K^*$  and  $\phi$  can also be used to explore collective flow and vorticity in nucleus-nucleus collisions. PHENIX has reported measurements of the  $v_2$  of  $\phi$  mesons in Cu+Au and U+U collisions [22]. The  $v_2(p_T)$  trends in the 0-20% most central Cu+Au collisions are consistent with those for the 0-30% most central Au+Au collisions, while  $v_2(p_T)$  for the 0-50% most central U+U collisions is consistent with mid-central (30-80%) Au+Au collisions. However, these various trends can be collapsed to essentially a single  $v_2(p_T)$  by scaling by the empirical factor  $\varepsilon N_{\text{part}}^{1/3}$ , where  $\varepsilon$  is the eccentricity of the nuclear overlap region.

Non-central A+A collisions have a large orbital angular momentum perpendicular to the reaction plane. This leads to vorticity in the QGP produced in the collision, which induces the global polarization of quarks in that QGP, which may be observable as a global polarization of the hadrons containing those quarks, including  $\Lambda$  baryons and  $K^*$  and  $\phi$  vector mesons. This polarization can be measured by finding the angular distributions of  $K^*$  and  $\phi$  decay products with respect to a suitable quantization axis (*e.g.*, the direction of the orbital angular momentum). From this, the elements of the spin-density matrix can be extracted. Deviations of the  $\rho_{00}$  spin-density matrix element from the unpolarized value of  $\frac{1}{3}$  indicated a net polarization of these mesons. STAR recently published such a study [23]. They observe  $\rho_{00}$  values consistent with  $\frac{1}{3}$  for Au+Au collisions at  $\sqrt{s_{NN}} = 200$  GeV. However, measurements for  $11.5 \leq \sqrt{s_{NN}} \leq 62$  GeV have  $\rho_{00} > \frac{1}{3}$  at the  $7.4\sigma$  level for the  $\phi$  meson. This result is supported by new STAR preliminary results from the second RHIC Beam Energy Scan [24]. It is also observed that  $\rho_{00}$  becomes larger and deviates even farther from  $\frac{1}{3}$ . This is consistent with expectations, since particles moving with larger rapidities encounter larger magnetic field fluctuations in the direction perpendicular to their motion. Earlier measurements by ALICE [25] indicate that at LHC energies,  $\rho_{00} < \frac{1}{3}$  for the  $K^*$ , using a lower  $p_T$  range than the STAR measurement. ALICE observes  $\rho_{00}$  consistent with the unpolarized value for vector mesons in  $p+p$  collisions and for  $K_S^0$  mesons (scalar particles) in A+A collisions.

I wish to thank the organizers for inviting me to give a presentation on this topic, and the many experimentalists and theorists whose work I have discussed here.

## References

- [1] S. Acharya et al. (ALICE), Evidence of rescattering effect in Pb–Pb collisions at the LHC through production of  $K^*(829)^0$  and  $\phi(1020)$  mesons, Phys. Lett. B **802**, 135225 (2020). [10.1016/j.physletb.2020.135225](https://doi.org/10.1016/j.physletb.2020.135225)
- [2] S. Acharya et al. (ALICE), System-size dependence of the hadronic rescattering effect at energies available at the CERN Large Hadron Collider, Phys. Rev. C **109**, 014911 (2024). [10.1103/PhysRevC.109.014911](https://doi.org/10.1103/PhysRevC.109.014911)
- [3] S. Singha (STAR),  $K^{*0}$  production in Ru+Ru and Zr+Zr collisions at  $\sqrt{s_{NN}} = 200$  GeV at RHIC, these proceedings (2024).
- [4] B. Kozłowski (NA61/SHINE),  $K^*/K$  ratio and the time between freeze-outs for intermediate-mass Ar+Sc system at the SPS energy range, these proceedings (2024).
- [5] S. Acharya et al. (ALICE), Multiplicity dependence of  $K^*(892)^0$  and  $\phi(1020)$  production in pp collisions at  $\sqrt{s} = 13$  TeV, Phys. Lett. B **807**, 135501 (2020). [10.1016/j.physletb.2020.135501](https://doi.org/10.1016/j.physletb.2020.135501)
- [6] A.G. Knospe et al., Hadronic resonance production and interaction in  $p$ –Pb collisions at LHC energies in EPOS3, Phys. Rev. C **104**, 054907 (2021). [10.1103/PhysRevC.104.054907](https://doi.org/10.1103/PhysRevC.104.054907)
- [7] A. Iñer et al., Probing hot and dense nuclear matter with  $K^*$ ,  $\bar{K}^*$  vector mesons, Phys. Rev. C **99**, 024914 (2019). [10.1103/PhysRevC.99.024914](https://doi.org/10.1103/PhysRevC.99.024914)

- [8] D. Oliinychenko, C. Shen, Resonance production in PbPb collisions at 5.02 TeV via hydrodynamics and hadronic afterburner, arXiv:2105.07539 (2021). [10.48550/arXiv.2105.07539](https://arxiv.org/abs/2105.07539)
- [9] V. Vovchenko, B. Dönigus, H. Stoecker, Canonical statistical model analysis of  $p$ - $p$ ,  $p$ -Pb, and Pb-Pb collisions at energies available at the CERN Large Hadron Collider, Phys. Rev. C **100**, 054906 (2019). [10.1103/PhysRevC.100.054906](https://arxiv.org/abs/1811.07371)
- [10] A. Motornenko et al., Kinetic freeze-out temperature from yields of short-lived resonances, Phys. Rev. C **102**, 024909 (2020). [10.1103/PhysRevC.102.024909](https://arxiv.org/abs/1908.07311)
- [11] S. Acharya et al. (ALICE),  $\Sigma(1385)^\pm$  resonance production in Pb-Pb collisions at  $\sqrt{s_{NN}}=5.02$  TeV, Eur. Phys. J. C **83**, 351 (2023). [10.1140/epjc/s10052-023-11475-1](https://arxiv.org/abs/2208.07311)
- [12] S. Acharya et al. (ALICE), Light-flavor particle production in high-multiplicity pp collisions at  $\sqrt{s} = 13$  TeV as a function of transverse sphericity, J. High Energy Phys. **05**, 184 (2024). [10.1007/JHEP05\(2024\)184](https://arxiv.org/abs/2401.11844)
- [13] S. Acharya et al. (ALICE), Multiplicity dependence of light-flavor hadron production in pp collisions at  $\sqrt{s} = 7$  TeV, Phys. Rev. C **99**, 024906 (2019). [10.1103/PhysRevC.99.024906](https://arxiv.org/abs/1808.07311)
- [14] L. Rozpłochowski (NA61/SHINE), Energy dependence of  $\phi(1020)$  meson production in nucleus-nucleus collisions at the CERN SPS, these proceedings (2024).
- [15] M. Lorenz (HADES), HADES highlights: Recent results from HADES, these proceedings (2024).
- [16] S. Acharya et al. (ALICE),  $f_0(980)$  production in inelastic pp collisions at  $\sqrt{s} = 5.02$  TeV, Phys. Lett. B **846**, 137644 (2023). [10.1016/j.physletb.2022.137644](https://arxiv.org/abs/2208.13764)
- [17] S. Acharya et al. (ALICE), Observation of abnormal suppression of  $f_0(980)$  production in p-Pb collisions at  $\sqrt{s_{NN}} = 5.02$  TeV, Phys. Lett. B **853**, 138665 (2024). [10.1016/j.physletb.2024.138665](https://arxiv.org/abs/2401.13865)
- [18] A. Hayrapetyan et al. (CMS), Elliptic anisotropy measurement of the  $f_0(980)$  hadron in proton-lead collisions and evidence for its quark-antiquark composition, arXiv:2312.17092 (2023). [10.48550/arXiv.2312.17092](https://arxiv.org/abs/2312.17092)
- [19] P. Das (ALICE), Investigating the hidden strangeness content of exotic resonance with ALICE, these proceedings (2024).
- [20] S. Acharya et al. (ALICE),  $K_S^0 K_S^0$  and  $K_S^0 K^\pm$  femtoscopy in pp collisions at  $\sqrt{s} = 5.02$  and 13 TeV, Phys. Lett. B **833**, 137335 (2022). [10.1016/j.physletb.2022.137335](https://arxiv.org/abs/2208.13733)
- [21] S. Acharya et al. (ALICE), Investigating the composition of the  $K_0^*(700)$  state with  $\pi^\pm K_S^0$  correlations at the LHC, Phys. Lett. B **856**, 138915 (2024). [10.1016/j.physletb.2024.138915](https://arxiv.org/abs/2401.13891)
- [22] N.J. Abdulameer et al. (PHENIX), Measurement of  $\phi$ -meson production in Cu+Au collisions at  $\sqrt{s_{NN}} = 200$  GeV and U+U collisions at  $\sqrt{s_{NN}} = 193$  GeV, Phys. Rev. C **107**, 014907 (2023). [10.1103/PhysRevC.107.014907](https://arxiv.org/abs/2208.01490)
- [23] M.S. Abdallah et al. (STAR), Pattern of global spin alignment of  $\phi$  and  $K^{*0}$  mesons in heavy-ion collisions, Nature **614**, 244 (2023). [10.1038/s41586-022-05557-5](https://arxiv.org/abs/2308.01490)
- [24] G. Wilks (STAR), Differential measurements of  $\phi$ -meson global spin alignment in Au+Au collisions at STAR, these proceedings (2024).
- [25] S. Acharya et al. (ALICE), Evidence of spin-orbital angular momentum interactions in relativistic heavy-ion collisions, Phys. Rev. Lett. **125**, 012301 (2020). [10.1103/PhysRevLett.125.012301](https://arxiv.org/abs/1908.01230)